RADIATION AND HEAT GENERATION EFFECTS IN MAGNETOHYDRODYNAMIC MIXED CONVECTION FLOW OF NANOFLUIDS

by

Aaiza GUL[a], Ilyas KHAN[a,b,*], and Sharidan SHAFIE[a]

[a] Department of Mathematical Sciences, Faculty of Science,
University of Technology Malaysia, UTM Skudai, Malaysia
[b] Basic Sciences Department, College of Engineering, Majmaah University, Majmaah, Saudi Arabia

Original scientific paper
https://doi.org/10.2298/TSCI150730049G

Radiation and heat generation effects in unsteady magnetohydrodynamic mixed convection flow of nanofluids along a vertical channel are investigated. Silver nanoparticles of spherical shapes and of different sizes in water as a convectional base fluid are incorporated. The purpose of this study is to measure the effect of different sizes of nanoparticles on velocity and temperature. Keeping in mind the size, particle material, shape, clustering and Brownian motion of nanoparticles, Koo and Kleinstreuer model is used. The problem is modeled in terms of partial differential equations with physical boundary conditions. Analytical solutions are obtained for velocity and temperature, plotted and discussed. It is concluded that increasing the size of Ag nanoparticles (up to specific size, 30 nm, results in a very small velocity increment while for large particle size (30-100 nm), no change in velocity is observed. As the small size of nanoparticles has the highest thermal conductivity and viscosity. This change in velocity with size of nanoparticles is found only in water-based nanofluids with low volume fraction 0.01 while at low volume concentration, no change is observed.

Key words*: radiation, heat generation, magnetohydrodynamic mixed convection, spherical Ag nanofluids, analytical solutions*

Introduction

Heat transfer due to mixed convection with radiation and heat generation effects is of great significance in many industrial processes such as heating and cooling. This mode of heat transfer can be sufficiently enhanced by changing either flow geometry or boundary conditions, or due to fluid thermo-physical properties. An innovative way of improving the thermal conductivity of the fluid is to suspend small solid particles within it. At the beginning, this idea was limited only to particles with dimensions of the order of micrometers [1]. Hamilton and Crosser [2] extended the Maxwell model in order to take into account the effect of the different shapes of the solid particles for volume fraction less than 0.1. Both Maxwell [1] and Hamilton and Crosser [2] models were derived for the suspension of micro-or milli-sized solid particles inside the fluids. But frequently, these models were utilized due to their simplicity in the study of nanofluids. Then later on, in 1995, Choi [3] extended this idea to nanometer-sized particles and dispersed them within a base fluid such as water.

* Corresponding author, e-mail: i.said@mu.edu.sa

These types of suspensions, he named as nanofluids. Different novel characteristics of nanofluids make them strongly applicable in different processes of heat transfer. Examples of such processes include fuel cells, microelectronics, hybrid-powered engines, and pharmaceutical applications [4-6].

Yu and Choi [7] modified the Maxwell model [1] by including the effect of the liquid nanolayers formed around nanoparticles. In another investigation, Yu and Choi [8] extended this idea by modifying the Hamilton and Crosser model for non-spherical particles. Several other models were also introduced to take into account different effects of nanoparticles. For example, Xuan *et al.* [9] presented their own model by considered the effect of Brownian motion, size and clustering of nanoparticles. They considered the thermal conductivity of nanofluids to be composed of two parts; static part represents the thermal conductivity enhancement due to the higher thermal conductivity of the nanoparticles and second part takes the effect of Brownian motion into account. Koo and Kleinstreuer [10] proposed a model by taking into account the effect of Brownian motion of nanoparticles. They also considered the thermal conductivity of nanofluids to be composed of two parts as Xuan *et al.* [9] considered. They also calculated some parameters by using experimental data of Das *et al.* [11] for CuO nanofluid. Thermal conductivity of Al_2O_3/water nanofluid was experimentally investigated by Chon *et al.* [12]. He also proposed a correlation for the determination of the thermal conductivity of alumina nanofluids based on the experimental data. Though several attempts have been made on nanofluids to explain the physical reasons for the heat transfer enhancement [13, 14], there are still many conspicuous inconsistencies and the investigators are working on, see for example some recent attempts in [15-33].

Earlier studies indicate that no exact analysis has been made so far for the radiation and heat generation effects on nanofluids. Therefore, present study aims to investigate the effects of radiation and heat generation on unsteady mixed convection flow of nanofluids along a vertical channel with induced magnetic field and external pressure gradient. Silver nanoparticles of spherical shapes and of different sizes in water as a convectional base fluid are incorporated. Solutions for velocity and temperature are plotted and discussed for different embedded parameters. Influence of different sizes of nanoparticles on velocity and temperature is investigated.

Problem formulation and solution

In this problem, water-based nanofluid containing magnetite (Ag and Al_2O_3) nanoparticles is considered. Pressure gradient of oscillatory type is applied in the flow direction. Radiation and heat generation effects are taken into account. Mixed convection flow is induced inside a vertical channel of width d with constant temperature. Fluid is electrically conducting due to magnetic field $\vec{\mathrm{B}}_0$ of strength B_0 applied in a transverse direction to the flow. Magnetic Reynolds number is taken small and induced magnetic field is neglected. External electric field and electric field due to polarization is taken zero. One boundary of the channel is maintained at constant temperature T_w while other boundary has uniform temperature T_0. Channel is taken along x-axis and y-axis is taken normal to the flow direction. After using approximation of Boussinesq and taking into consideration the above assumptions, the governing equations of momentum and energy are obtained [31, 32]:

$$\rho_{\mathrm{nf}} \frac{\partial u}{\partial t} = -\frac{\partial p}{\partial x} + \mu_{\mathrm{nf}} \frac{\partial^2 u}{\partial y^2} - \sigma_{\mathrm{nf}} B_0^2 u + (\rho\beta)_{\mathrm{nf}} \mathrm{g}(T - T_\infty) \tag{1}$$

$$(\rho c_p)_{\mathrm{nf}} \frac{\partial T}{\partial t} = k_{\mathrm{nf}} \frac{\partial^2 T}{\partial y^2} + Q_0 (T - T_0) - \frac{\partial q}{\partial y} \tag{2}$$

with boundary conditions

$$u(0,t) = 0, \quad T(0,t) = T_0 \tag{3}$$

$$u(d,t) = 0, \quad T(d,t) = T_w \tag{4}$$

where $u = u(y, t)$ denotes the fluid velocity in the x-direction, $T = T(y, t)$ is the temperature of the nanofluid, ρ_{nf} – the density of the nanofluid, μ_{nf} – the dynamic viscosity of the nanofluid, σ_{nf} – the electrical conductivity of the nanofluid, $(\rho\beta)_{\mathrm{nf}}$ – the thermal expansion of the nanofluid, g – the acceleration due to gravity, c_p – the specific heat of the nanofluid at constant pressure, k_{nf} – the thermal conductivity of the nanofluid, and q – the radiative heat flux in x-direction.

The density ρ_{nf} thermal expansion coefficient $(\rho\beta)_{\mathrm{nf}}$ and heat capacitance $(\rho c_p)_{\mathrm{nf}}$ of nanofluids are derived by using the relations given by [13, 16, 17, 21].

$$\begin{gathered}(\rho c_p)_{\mathrm{nf}} = (1-\phi)(\rho c_p)_{\mathrm{f}} + (\rho c_p)_{\mathrm{s}}, \quad \rho_{\mathrm{nf}} = (1-\phi)\rho_{\mathrm{f}} + \phi\rho_{\mathrm{s}}, \quad k_{\mathrm{nf}} = \alpha_{\mathrm{nf}}(\rho c_p), \\ (\rho\beta)_{\mathrm{nf}} = (1-\phi)(\rho\beta)_{\mathrm{f}} + \phi(\rho\beta)_{\mathrm{s}}, \quad \sigma_{\mathrm{nf}} = \sigma_{\mathrm{f}}\left[1 + \frac{3(\sigma-1)\phi}{(\sigma+2)-(\sigma-1)\phi}\right], \quad \sigma = \frac{\sigma_{\mathrm{s}}}{\sigma_{\mathrm{f}}}\end{gathered} \tag{5}$$

where ϕ is the volume fraction of the nanoparticles, ρ_{f} and ρ_{s} are the density of the base fluid and solid nanoparticles, respectively, μ_{f} is the dynamic viscosity of the base fluid, k_{f} and k_{s} are the thermal conductivities of the base fluid and solid nanoparticles, respectively, $c_{p\mathrm{f}}$ and $c_{p\mathrm{s}}$ denote the specific heat at constant pressure corresponding to the base fluid and solid nanoparticles, respectively, σ_{f} and σ_{s} are the electrical conductivity of base fluid and solid nanoparticles, respectively. The total term ρc_p is known as heat capacitance. Some physical properties of nanoparticles and base fluid are listed in tab. 1 [13, 16, 17, 21]. These properties will be used in numerical computations of this problem.

Table 1. Thermo-physical properties of basefluids and nanoparticles

Model	c_p [$\mathrm{kg^{-1}K^{-1}}$]	ρ [$\mathrm{kgm^{-3}}$]	k [$\mathrm{Wm^{-1}K^{-1}}$]	$\beta \cdot 10^{-5}$ [$\mathrm{K^{-1}}$]	σ [$\mathrm{Sm^{-1}}$]
Water (H_2O)	4179	997.1	0.613	21	$5.5 \cdot 10^{-6}$
EG ($C_2H_6O_2$)	0.58	1.115	0.1490	6.5	$1.07 \cdot 10^{-6}$
Silver (Ag)	235	10500	429	1.89	$6.30 \cdot 10^{7}$
Alumina (Al_2O_3)	765	3970	40	0.85	$35 \cdot 10^{6}$

The effective thermal conductivity $k_{p\mathrm{f}}$ and viscosity $\mu_{p\mathrm{f}}$ of nanofluid are derived by using the generalized model of Koo and Kleinstreuer [10]:

$$k_{\mathrm{nf}} = k_{\mathrm{static}} + k_{\mathrm{Brownian}}$$

$$k_{\mathrm{nf}} = k_{\mathrm{f}}\left[\frac{(k_{\mathrm{s}} + 2k_{\mathrm{f}}) - 2\phi(k_{\mathrm{f}} - k_{\mathrm{s}})}{(k_{\mathrm{s}} + 2k_{\mathrm{f}}) + \phi(k_{\mathrm{f}} - k_{\mathrm{s}})}\right], \quad k_{\mathrm{Brownian}} = 5 \cdot 10^4 \beta\phi\rho_{\mathrm{f}} c_{p\mathrm{f}} \sqrt{\frac{k_{\mathrm{b}} T}{\rho_{\mathrm{s}} d_{\mathrm{p}}}} f(T, \phi, etc.) \tag{6}$$

$$\mu_{\mathrm{nf}} = \mu_{\mathrm{static}} + \mu_{\mathrm{Brownian}},$$
$$\mu_{\mathrm{static}} = \frac{\mu_f}{(1-\phi)^{2.5}}, \quad \mu_{\mathrm{Brownian}} = 5\cdot 10^4 \beta\phi\rho_{\mathrm{f}}\sqrt{\frac{k_{\mathrm{b}}T}{\rho_{\mathrm{s}}d_{\mathrm{p}}}} f(T,\phi,etc.) \tag{7}$$

where k_b is the Boltzman constant = $1.3807\cdot 10^{-23}$ J/K, T – the temperature of the nanofluids, 300 K > T > 325 K, d_p – the diameter of solid particles, β – the modelling function which is used to represents the fraction of the liquid volume, which travels with a particle. It is related to the particle motion. Here, $f(T, \phi, etc.)$ is function which depends on properties of intervening fluid and hence particle interactions. Interparticle potential has been used to take the interparticle interaction into consideration. It was difficult to find the theoretical value of $f(T, \phi, etc.)$. Therefore, experimental results of Das *et al.* [10] for Al_2O_3 and experimental results of Patel *et al.* [24] for Ag nanoparticles have been listed in tabs. 2 and 3. The values of these two functions, β and $f(T, \phi, etc.)$, are mentioned in tabs. 2 and 3 [10, 33]. Koo and Kleinstreuer [10] model is the generalized model of these two models.

Table 2. For β

Type of particles	β	Remarks
Ag	$0.0137(100\phi)^{-0.8229}$	$\phi < 1\%$
Al_2O_3	$0.0017(100\phi)^{-0.0841}$	$\phi > 1\%$

Table 3. For $f(T, \phi, etc.)$

Type of particles	$f(T, \phi, etc.)$
Ag	1
Al_2O_3	$(-64 + 0.4705)T + (1722.3\phi - 134.63)$

Therefore, the expressions in eqs. (6) and (7) are restricted only to spherical shape of nanoparticles. The radiative heat flux give:

$$-\frac{\partial q}{\partial y} = 4\alpha_0^2 (T - T_0) \tag{8}$$

where α_0 is the mean radiation absorption coefficient. Applied pressure gradient in the flow direction is taken as $-\partial p/\partial x = \lambda\exp(i\omega_1 t)$, where λ is constant and ω_1 – the frequency of oscillation. Introducing following dimensionless variables:

$$x^* = \frac{x}{d}, \quad y^* = \frac{y}{d}, \quad u^* = \frac{u}{U_0}, \quad t^* = \frac{tU_0}{d}, \quad P^* = \frac{d}{\mu U_0}p, \quad T^* = \frac{T - T_0}{T_w - T_0},$$
$$\omega^* = \frac{d\omega_1}{U_0}, \quad \frac{\partial p}{\partial x} = \lambda\varepsilon \mathrm{e}^{i\omega_1 t} \tag{9}$$

the system of eqs. (1)-(4) reduces to:

$$a_0 \frac{\partial u}{\partial t} = \lambda\varepsilon\exp(i\omega t) + \phi_2 \frac{\partial^2 u}{\partial y^2} - m_0^2 u + a_1 T \tag{10}$$

$$u(0,t) = 0, \quad u(1,t) = 0, \quad t > 0 \tag{11}$$

$$b_0^2 \frac{\partial T}{\partial t} = \frac{\partial^2 T}{\partial y^2} + b_1^2 T \tag{12}$$

$$T(0,t) = 0, \quad T(1,t) = 1, \quad t > 0 \tag{13}$$

where

$$a_0 = \phi_1 \,\mathrm{Re}, \quad \phi_1 = (1-\phi) + \phi\frac{\rho_\mathrm{s}}{\rho_\mathrm{f}}, \quad \mathrm{Re} = \frac{U_0 d}{\nu},$$

$$\phi_2 = \frac{1}{(1-\phi)^{2.5}} + \frac{5\cdot 10^4 \beta\phi\rho_\mathrm{f}}{\mu_\mathrm{f}}\sqrt{\frac{k_\mathrm{b}T}{\rho_\mathrm{s}d_\mathrm{p}}}f(T,\phi,etc.), \quad m_0^2 = \phi_5 M^2, \quad \phi_5 = \left[1 + \frac{3(\sigma-1)\phi}{(\sigma+2)-(\sigma-1)\phi}\right],$$

$$M^2 = \frac{\sigma_\mathrm{f} B_0^2 d^2}{\mu}, \quad a_1 = \phi_3 \,\mathrm{Gr}, \quad \phi_3 = (1-\phi)\rho_\mathrm{f} + \phi\frac{(\rho\beta)_\mathrm{s}}{\beta_\mathrm{f}}, \quad \mathrm{Gr} = \frac{g\beta_\mathrm{f} d^2 (T_w - T_0)}{\nu_\mathrm{f} U_0},$$

$$b_0{}^2 = \frac{\mathrm{Pe}\phi_4}{\lambda_n}, \quad \phi_4 = \left[(1-\phi) + \phi\frac{(\rho c_p)_\mathrm{s}}{(\rho c_p)_\mathrm{f}}\right], \quad \mathrm{Pe} = \frac{U_0 d(\rho c_p)_\mathrm{f}}{k_\mathrm{f}},$$

$$\lambda_\mathrm{n} = \frac{k_\mathrm{nf}}{k_\mathrm{f}} = \left[\frac{(k_\mathrm{s}+2k_\mathrm{f}) - 2\phi(k_\mathrm{f}-k_\mathrm{s})}{(k_\mathrm{s}+2k_\mathrm{f}) + \phi(k_\mathrm{f}-k_\mathrm{s})}\right] + 5\cdot 10^4 \beta\phi\rho_\mathrm{f} c_{p\mathrm{f}}\sqrt{\frac{k_\mathrm{b}T}{\rho_\mathrm{s}d_\mathrm{p}}}f(T,\phi,etc.),$$

$$b_1 = \frac{1}{\lambda_n}(Q + N^2), \quad Q = \frac{d^2 Qo}{k_\mathrm{f}}, \quad N^2 = \frac{4d^2\alpha_0^2}{k_\mathrm{f}}$$

Here Re*, M,* Gr, Pe*, Q,* and *N* denote the Reynold's number, magnetic parameter, the thermal Grashof number, the Peclet number, heat generation, and the radiation parameter, respectively.

In order to solve eqs. (10)-(13) the following perturbed type solutions are assumed:

$$u(y,t) = \left[u_0(y) + \varepsilon\exp(i\omega t)u_1(y)\right] \tag{14}$$

$$T(y,t) = \left[T_0(y) + \varepsilon\exp(i\omega t)T_1(y)\right] \tag{15}$$

Using eqs. (14) and (15) into eqs. (10)-(13), respectively, the following system of ordinary differential equations is obtained:

$$\frac{\mathrm{d}^2 u_0(y)}{\mathrm{d}y^2} - m_1^2 u_0(y) = -a_2 T_0(y) \tag{16}$$

$$u_0(0) = 0, \quad u_0(1) = 0 \tag{17}$$

$$\frac{\mathrm{d}^2 u_1(y)}{\mathrm{d}y^2} - m_2^2 u_1(y) = -\frac{\lambda}{\phi_2} \tag{18}$$

$$u_1(0) = 0, \quad u_1(1) = 0 \tag{19}$$

$$\frac{\mathrm{d}^2 T_0(y)}{\mathrm{d}y^2} - b_1^2 T_0(y) = 0 \tag{20}$$

$$T_0(0) = 0, \quad T_0(1) = 0 \tag{21}$$

$$\frac{\mathrm{d}^2 T_1(y)}{\mathrm{d}y^2} + m_3^2 T_1(y) = 0 \tag{22}$$

$$T_1(0) = 0, \quad T_1(1) = 0 \tag{23}$$

where

$$m_1 = \sqrt{\frac{m^2{}_0}{\phi_2}}, \quad a_2 = \frac{a_1}{\phi_2}, \quad m_2 = \sqrt{\frac{m_0^2 + i\omega a_0}{\phi_2}}, \quad m_3 = \sqrt{b_1 - i\omega b_0}$$

Solutions of eqs. (20)-(23) yield:

$$T_0(y) = \frac{\sin(b_1 y)}{\sin(b_1)} \tag{24}$$

$$T_1(y) = 0 \tag{25}$$

Now eq. (15), after using eqs. (24) and (25) becomes:

$$T(y,t) = T(y) = \frac{\sin(b_1 y)}{\sin(b_1)} \tag{26}$$

Incorporate eq. (26) into eq. (16) and then the solution of the resulting equation with boundary conditions (17) yields:

$$u_0(y) = c_1 \sinh(m_1 y) + c_2 \cosh(m_1 y) + \frac{a_2}{(b_1^2 + m_1^2)} \frac{\sin(b_1 y)}{\sin(b_1)} \tag{27}$$

Similarly, eq. (18) with boundary conditions (19) results in:

$$u_1(y) = c_3 \sinh(m_2 y) + c_4 \cosh(m_2 y) + \frac{\lambda}{m_2^2 \phi_2} \tag{28}$$

Here c_1, c_2, c_3, and c_4 are arbitrary constants given by:

$$c_1 = -\frac{a_2}{\sinh(m_1)(b_1^2 + m_1^2)}, \quad c_2 = 0, \quad c_3 = \frac{\lambda}{m_2^2 \phi_2} \frac{1}{\sinh(m_2)} [\cosh(m_2) - 1], \quad c_4 = -\frac{\lambda}{m_2^2 \phi_2}$$

Now using eqs. (27) and (28) into eq. (16), give:

$$u(y,t) = -\frac{a_2 \sinh(m_1 y)}{(b_1^2 + m_1^2)\sinh(m_1)} + \frac{a_2 \sin(b_1 y)}{(b_1^2 + m_1^2)\sin(b_1)} +$$
$$+\varepsilon \exp(i\omega t)\left\{\frac{\lambda[\cosh(m_2) + 1]\sinh(m_2 y)}{m_2^2 \phi_2 \sinh(m_2)} - \frac{\lambda}{m_2^2 \phi_2}[\cosh(m_2 y) - 1]\right\} \tag{29}$$

Nusselt number and skin-friction

Nusselt number and skin-friction are evaluated from eqs. (26) and (29) as:

$$\mathrm{Nu} = \frac{b_1}{\sin(b_1)} \tag{30}$$

$$\tau_1 = \tau_1(t) = -\frac{a_2 m_1}{(b_1^2 + m_1^2)\sinh(m_1)} + \frac{a_2 b_1}{(b_1^2 + m_1^2)\sin(b_1)} + \varepsilon \exp(i\omega t) \frac{\lambda m_2 [\cosh(m_2) - 1]}{m_2^2 \phi_2 \sinh(m_2)} \tag{31}$$

Results and discussion

Graphical results with illustration are included in this section. Koo and Kleinstreuer [10] model is used to derive velocity profile of silver-water based nanofluids. Using the thermophysical properties H_2O, $C_2H_6O_2$, Ag, and Al_2O_3 from tab. 1, figs. 1-11 are plotted. In these figs. 1-6 and 10 are sketched for velocity profiles, and 7-9 and 11 for temperature profiles. Figure 1 is sketched to show velocity profile of Ag nanoparticles of different sizes in water-based nanofluids. One can see from this fig. 1 that on increasing size of Ag nanoparticles (from 1 nm to 30 nm) in water-based nanofluids, velocity is found to increase. However, after 30 nm, no variation is observed, even if the size of nanoparticle is increased upto 100 nm or above. Only a small variation is observed when volume fraction of nanofluids is taken as 0.01.

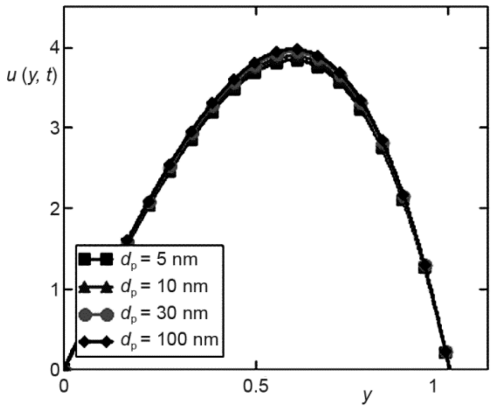

Figure 1. Velocity graph for different sizes of Ag in water-based nanofluid when Gr = 0.1, N = 0.1, Re = 1, Pe = 1, M = 1, λ = 1, t = 0.1, and Q = 0.001, ϕ = 0.01, ω = 0.2

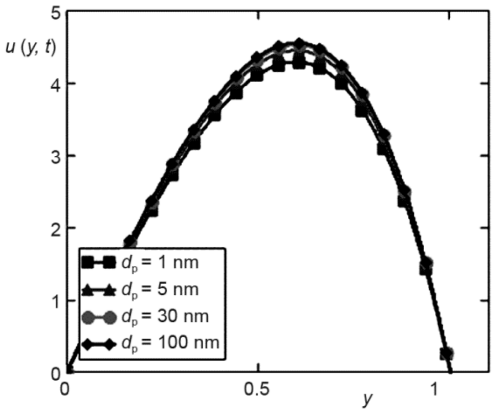

Figure 2. Velocity graph for different sizes of Al_2O_3 in water-based nanofluid when ϕ = 0.01, Q = 0.01, Gr = 0.1, N = 0.1, Re = 1, Pe = 1, M = 1, λ = 1, t = 0.1, and ω = 0.2

This result shows that size of Ag nanoparticles is effected in very small volume fraction. The increasing of velocity with size of nanoparticle means that viscosity and thermal conductivity of nanofluids are decreasing. It is clear from fig. 1 that dispersion of Ag nanoparticles of small sizes show higher viscosity and thermal conductivity. According to theory of Brownian motion, random motion of small size particles is greater than large size particles or aggregation and aggregate containing a number of nanoparticles or clusters slow down the random motion of nanoparticles. This means that large size particles has greater possibility of making clusters as compare to small size particles. Therefore, suspension of small size particles has greater thermal conductivity. However, after a certain increase of size no variation is observed. It is also mention in Xuan *at el.* [9] model that smaller the radius of aggregation or cluster of suspended nanoparticles higher will be thermal conductivity of nanofluids and completed dispersed single particles (without aggregation or cluster) is found only in an ideal case.

Figure 2 is sketched to represent velocity profile of Al_2O_3 in water-based nanofluids. This figure shows that dispersion of Al_2O_3 nanoparticles in water gives the same results as found in case of dispersion of Ag nanoparticles in water-based nanofluids. But variation in velocity of Al_2O_3 nanoparticles in water-based nanofluids is found only at high volume fraction. Although variation in velocity of dispersion of Ag nanoparticles in water is found at low volume concentration. This means that ϕ plays an important role when the size of Ag nanoparticle is kept constant in both cases of water-based nanofluid and Al_2O_3 based-nanfluid. It is

also important to note that there is a limit of adding nanoparticles to the base fluid. Physically, it is due to the sedimentation in nanofluids by high volume concentration taken at different volume for different nanoparticles.

Graphical results of dispersion of different sizes of Ag in EG-based nanofluids are shown in fig. 3. It is found from this figure that there is no variation in velocity with size of nanoparticles in EG-based nanofluids. It means that the size is unaffected in EG-based nanofluids even at a high ϕ. Comparison of Ag and Al_2O_3 in water-based nanofluids is shown in fig. 4. It is noted that Al_2O_3 in water-based nanofluids has high velocity as compare to Ag in water-based nanofluids. This means that silver is more viscous than Al_2O_3 in water-based nanofluids. Figure 5 is drawn to represent the velocity profile for different ϕ. It is noted from this figure that with the increase of ϕ velocity of nanofluids decreases. This physically means that with the increase of ϕ viscosity of nanofluids increases, due to which velocity of nanofluids decreases. Figure 6 is sketched to show the velocity profile for different value of Q. It is found from fig. 6 that velocity of nanofluids increases with the increase of Q.

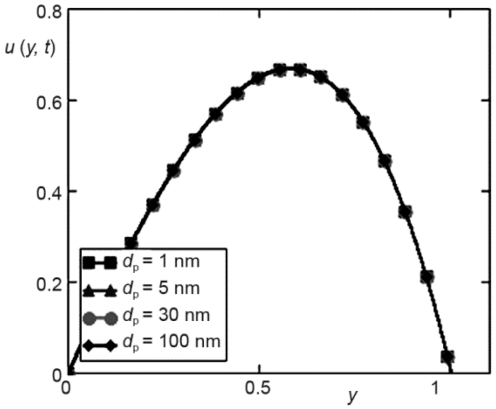

Figure 3. Velocity graph for different sizes of Ag in EG-based nanofluid when ϕ = 0.1, Q = 0.01, Gr = 0.1, N = 0.1, Re = 1, Pe = 1, λ = 1, t = 0.1, and ω = 0.2

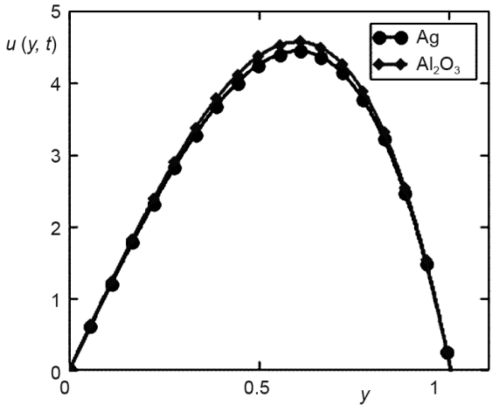

Figure 4. Velocity comparison graph of Ag and Al_2O_3 in water based nanofluids when Q = 0.01, d_p = 5 nm, Gr = 0.1, N = 0.1, Re = 1, Pe = 1, λ = 1, t = 0.1, and ω = 0.2

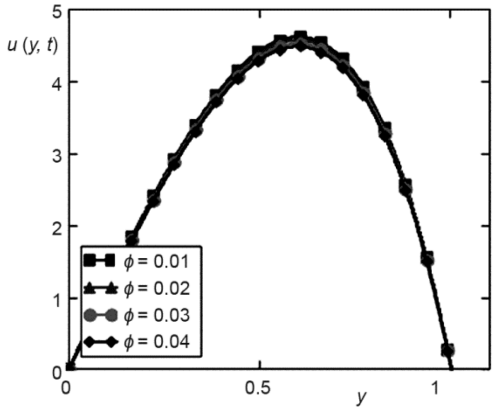

Figure 5. Velocity profile of Ag nanofluid for different ϕ when Q = 0.01, d_p = 5 nm, Ag, Gr = 0.1, N = 0.1, Re = 1, Pe = 1, λ = 1, t = 0.1, and ω = 0.2

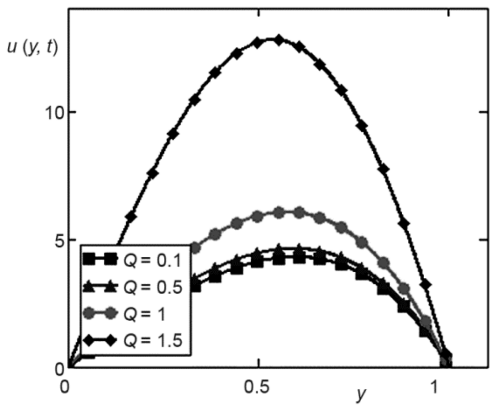

Figure 6. Velocity graph for different values of Q when ϕ = 1, Q = 0.01, d_p = 5 nm, Ag, Gr = 0.1, N = 0.1, Re = 1, Pe = 1, λ = 1, t = 0.1, and ω = 0.2

Graphs of temperature profile for different values of radiation parameter N volume fraction, and heat generation parameter are given in figs. 7-9 and 11. Figure 7 on the other hand indicates that temperature of nanofluids increases with the increase of ϕ but this variation in temperature is observed at very high ϕ for Ag in water-based nanofluids. This is due to the reason that with the increase of volume fraction, thermal conductivity and viscosity increase but the variation in thermal conductivity lead to increase the temperature of nanofluids and viscosity start decreasing with increasing temperature. Figure 8 shows that temperature profiles of nanofluids increase with the increase of radiation parameter N. This physically means that an increase in radiation parameter, increases the rate of heat energy transport to the fluid. Increasing rate of heat transfer decreases the viscosity of nanofluids due to which temperature of nanofluids increases. When $N = 0$, means there is no radiation from the fluid. This physically means the nanofluid has low temperature. Figure 9 represents temperature profile for different value of Q. It is clear from this figure that nanofluids temperature increases with the increase of Q.

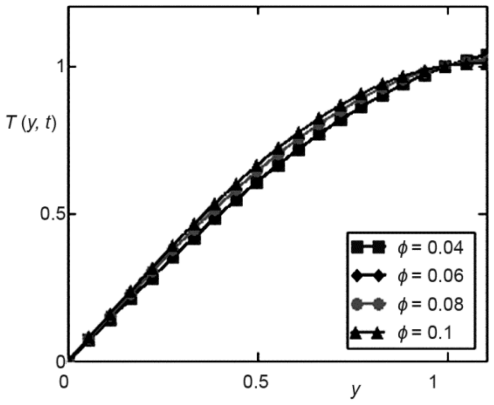

Figure 7. Velocity profile for different value of ϕ when $Q = 1$, $d_p = 5$ nm, Ag, Gr = 0.1, $N = 0.1$, Re = 1, Pe = 1, $\lambda = 1$, $t = 0.1$, and $\omega = 0.2$

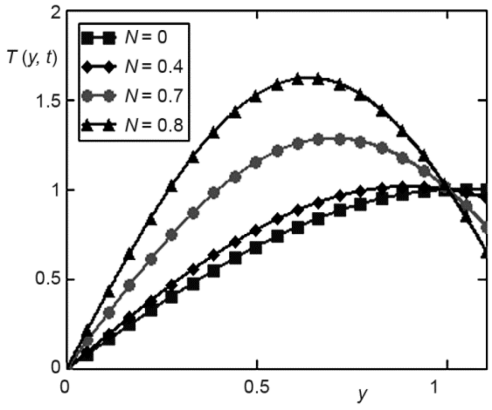

Figure 8. Temperature profile for different value of radiation parameter N when $\phi = 0.04$, $Q = 1$, $t = 1$, and $d_s = 5$ nm

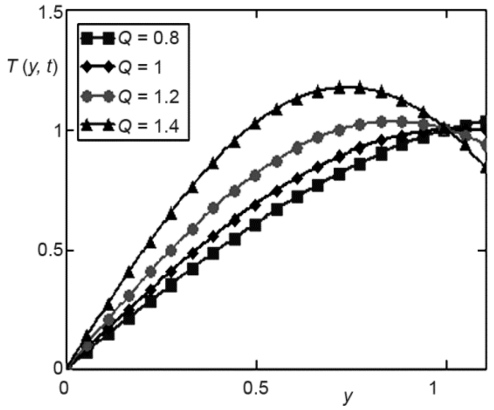

Figure 9. Temperature profile for different value of volume fraction Q when $t = 1$, $N = 0.1$, $\phi = 0.04$, $d_s = 5$ *nm*

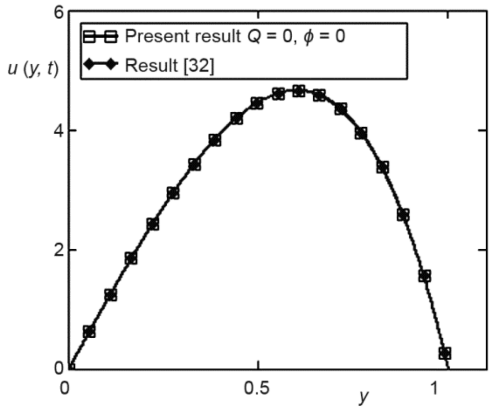

Figure 10. Comparison of present velocity results when $\phi = 0$, $Q = 0$, with published results [32]

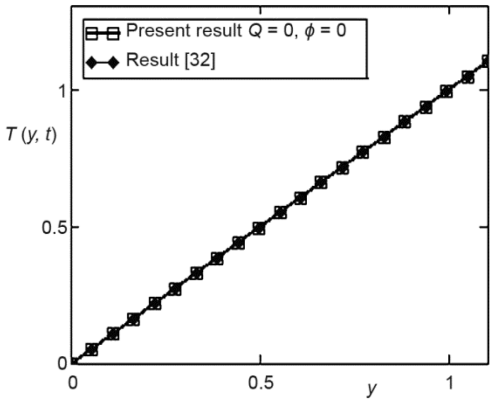

Figure 11. Comparison of present tempertaure results when $\phi = 0$, $Q = 0$, with published results [32]

Finally, in figures 10 and 11, the results of the present study are compared with those of Makinde and Mhone [32] in the absence of heat generation and in a non-porous medium. It can clearly be seen that the present results of velocity and temperature are identical with the results obtained for a regular fluid [32].

Final conclusions

In this work we have studied analytically heat transfer in mixed convection flow of MHD nanofluids inside a vertical channel with radiation and heat generation effects. The dispersion of different sizes of Ag and Al_2O_3 nanoparticles in water as conventional base fluids is considered. In addition, the suspension of different sizes of Ag nanoparticles in EG-based nanofluids is also studied. Present result is compared with the existing result of Makinde [32] result and found an excellent agreement tab. 4. Expression for velocity and temperature are obtained. Results are plotted and the following conclusions are drawn.

- The suspension of small size nanoparticles (Ag and Al_2O_3) in water-based nanofluids has greater viscosity and thermal conductivity.
- It is also observed that there is a certain limit of increasing size of nanoparticles (upto 30 nm) which causes the velocity to increase and thereafter no change is observed for further increasing size of nanoparticles.
- It is found that there is certain limit of ϕ where size of nanoparticles start affecting. The size of Ag nanoparticles is affected only at small volume fraction (ϕ) 0.01 as compared to Al_2O_3 nanoparticles, size has no effect at this volume fraction on velocity of nanofluid but at high volume fraction 0.1, velocity of nanofluids start affecting with increasing size of Al_2O_3 nanoparticles. On the other side for EG-based nanofluids the size has no effect.
- Besides, velocity is decreasing with increase of ϕ due to viscosity increases whereas velocity is increasing with the increase of Q.
- In limiting sense the present results are reduced to published results [32].

Table 4. Comparison of present result with those of Makinde and Mhone [32]

	Present results	Present results when $Q = 0$ and $\phi = 0$	Makinde and Mhone [32] results in the absence of porous medium
Velocity	5.323	0.119	0.119
Temperature	0.501	0.599	0.599

Nomenclature

$\vec{B}_0$ – applied magnetic field, [T]
$(c_p)_f$ – heat capacity of base fluid, [$kg^{-1}K^{-1}$]
$(c_p)_{nf}$ – heat capacity of nanofluids, [$kg^{-1}K^{-1}$]
$(c_p)_s$ – heat capacity of solid nanoparticles, [$kg^{-1}K^{-1}$]
d_p – diameter of solid nanoparticles, [m]
$\vec{E}$ – total electric field, [NC^{-1}]
Gr – thermal Grashof number, [–]
g – gravitational acceleration, [ms^{-2}]
k_f – thermal conductivity of base fluid, [$Wm^{-1}K^{-1}$]

k_{nf} – thermal conductivity of nanofluids, [$Wm^{-1}K^{-1}$]
k_s – thermal conductivity of solid nanoparticles, [$Wm^{-1}K^{-1}$]
M – magnetic parameter, [–]
N – radiation parameter, [–]
Nu – Nusselt number, [–]
Pe – Peclet number, [–]
Q – heat generation parameter, [–]
T – temperature of nanofluids, [K]
t – time, [s]

Greek symbols

α_0 – mean absorption coefficient, [m^{-1}]
β_f – volumetric coefficient of thermal expansion of base fluid, [K^{-1}]
β_{nf} – volumetric coefficient of thermal expansion of nanofluids, [K^{-1}]
β_s – volumetric coefficient of thermal expansion of solid nanoparticles, [K^{-1}]
μ_f – dynamic viscosity of base fluid, [$kgm^{-1}s^{-1}$]
μ_m – magnetic permeability, [$H^{-1}m^{-1}$]
μ_{nf} – dynamic viscosity of solid nanofluids, [$kgm^{-1}s^{-1}$]
μ_s – dynamic viscosity of solid nanoparticles, [$kgm^{-1}s^{-1}$]
ρ_{nf} – density of nanofluids, [kgm^{-3}]
ρ_f – density of base fluid, [kgm^{-3}]
ρ_s – density of solid nanoparticles, [kgm^{-3}]
σ_s – electrical conductivity of nanofluids, [$\Omega^{-1}m^{-1}$(mho)]
$\boldsymbol{\tau}$ – viscous stress tensor, [Nm^{-2}]
τ_1 – skin friction, [–]
ω – oscillating parameter, [s^{-1}]
ϕ – volume fraction of solid nanoparticles, [–]

Acknowledgment

The author acknowledge with thanks the Deanship of Scientific Research at Majmaah University, Majmaah Saudi Arabia for technical and financial support through vote number 37/97 for this research project.

References

[1] Maxwell, J. C., *A Treatise on Electricity and Magnetism*, Clarendon Press Series, Clarendon Press, Oxford, UK, 1873, 2 v
[2] Hamilton, R., Crosser, O., Thermal Conductivity of Heterogeneous Two-Component Systems, *Industrial & Engineering Chemistry Fundamentals*, *1* (1962), 3, pp. 187-191
[3] Choi, S., Enhancing Thermal Conductivity of Fluids with Nanoparticles, ASME-Publications-Fed, 231 (1995), pp. 99-106
[4] Sheikholeslami, M., *et al.*, Simulation of MHD CuO-Water Nanofluid Flow and Convective Heat Transfer Considering Lorentz Forces, *Journal of Magnetism and Magnetic Materials*, *369* (2014), Nov., pp. 69-80
[5] Mohyud-Din, S. T., *et al.*, Magnetohydrodynamic Flow and Heat Transfer of Nanofluids in Stretchable Convergent/Divergent Channels, *Applied Sciences*, *5* (2015), 4, pp. 1639-1664
[6] Al-Salem, K., *et al.,* Effects of Moving Lid Direction on MHD Mixed Convection in a Linearly Heated Cavity*, International Journal of Heat and Mass Transfer*, *55* (2012), 4, pp. 1103-1112
[7] Yu, W., Choi, S., The Role of Interfacial Layers in the Enhanced Thermal Conductivity of Nanofluids: a Renovated Maxwell Model*, Journal of Nanoparticle Research*, *5* (2003), 1-2, pp. 167-171
[8] Yu, W., Choi, S., The Role of Interfacial Layers in the Enhanced Thermal Conductivity of Nanofluids: a Renovated Hamilton-Crosser model, *Journal of Nanoparticle Research*, *6* (2004), 4, pp. 355-361
[9] Xuan, Y., *et al.*, Aggregation Structure and Thermal Conductivity of Nanofluids*, AIChE Journal, 49* (2003), 4, pp. 1038-1043
[10] Koo, J., Kleinstreuer, C., A New Thermal Conductivity Model for Nanofluids*, Journal of Nanoparticle Research, 6* (2004), 6, pp. 577-588
[11] Das, S. K., *et al.,* Temperature Dependence of Thermal Conductivity Enhancement for Nanofluids*, Journal of Heat Transfer*, *125* (2003), 4, pp. 567-574
[12] Chon, C. H., *et al.,* Empirical Correlation Finding the Role of Temperature and Particle Size for Nanofluid (Al_2O_3) Thermal Conductivity Enhancement, *Applied Physics Letters, 87* (2005), 15, pp. 153107-153107
[13] Qasim, M., *et al.*, Mhd Boundary Layer Slip Flow and Heat Transfer of Ferrofluid along a Stretching Cylinder with Prescribed Heat Flux, *PloS One, 9* (2014), https://doi.org/10.1371/journal.pone.0083930
[14] Khan, Z. H., *et al.,* MHD Stagnation Point Ferrofluid Flow and Heat Transfer Toward a Stretching Sheet, Nanotechnology, *IEEE Transactions*, *13* (2014), 1, pp. 35-40

[15] Sheikholeslami, M., Ganji, D. D., Ferrohydrodynamic and Magnetohydrodynamic Effects on Ferrofluid Flow and Convective Heat Transfer, *Energy, 75* (2014), Oct., pp. 400-410
[16] Turkyilmazoglu, M., Unsteady Convection Flow of Some Nanofluids Past a Moving Vertical Flat Plate with Heat Transfer, *Journal of Heat Transfer*, *136* (2014), 3, ID 031704
[17] Asma, K., *et al.,* Exact Solutions for Free Convection Flow of Nanofluids, with Ramped Wall Temperature, *The European Physical Journal Plus*, *130* (2015), Apr., pp. 57-71
[18] Tiwari, A. K., *et al.,* Investigation of Thermal Conductivity and Viscosity of Nanoflurids, *J. Environ. Res. Develop*, *7* (2012), 2, pp. 768-777
[19] Zeeshan, A., *et al.,* Magnetohydrodynamic Flow of Water/Ethylene Glycol Based Nanofluids with Natural Convection through a Porous Medium, *The European Physical Journal Plus*, *129* (2014), 12, pp. 1-10
[20] Akbar, N. S., *et al.,* Impulsion of Induced Magnetic Field for Brownian Motion of Nanoparticles in Peristalsis, *Applied Nanoscience*, *6* (2015), 3, pp. 359-370
[21] Das, S., Jana, R. N., Natural Convective Magneto-Nanofluid Flow and Radiative Heat Transfer Past a Moving Vertical Plate, *Alexandria Engineering Journal*, *54* (2015), 1, pp. 55-64
[22] Garoosi, F., *et al.,* Two Phase Simulation of Natural Convection and Mixed Convection of the Nanofluid in a Squarecavity, *Powder Technology*, *275* (2015), May, pp. 239-256
[23] Sheikholeslami, M., Rashidi, M., Ferrofluid Heat Transfer Treatment in the Presence of Variable Magnetic Field, *The European Physical Journal Plus*, *130* (2015), 6, pp. 1-12
[24] Patel, H. E., *et al.,* Thermal Conductivities of Naked and Monolayer Protected Metal Nanoparticle Based Nanofluids: Manifestation of Anomalous Enhancement and Chemical Effects, *Applied Physics Letters*, *83* (2003), 14, pp. 2931-2933
[25] Brinkman, H., The Viscosity of Concentrated Suspensions and Solutions, *The Journal of Chemical Physics*, *20* (1952), 4, pp. 571-571
[26] Khan, U., *et al.,* Thermo-Diffusion, Diffusion-Thermo and Chemical Reaction Effects on MHD Flow of Viscous Fluid in Divergent and Convergent Channels, *Chemical Engineering Science*, *141* (2016), Feb., pp. 17-27
[27] Ahmed, N., *et al.*, MHD Flow of an Incompressible Fluid through Porous Medium between Dilating and Squeezing Permeable Walls, *Journal of Porous Media*, *17* (2014), 10, pp. 861-867
[28] Sheikholeslami, M., Ellahi, R., Three Dimensional Mesoscopic Simulation of Magnetic Field Effect on Natural Convection of Nanofluid, *International Journal of Heat and Mass Transfer*, *89* (2015), Oct., pp. 799-808
[29] Mohyud-Din, S. T., *et al.,* On Heat and Mass Transfer Analysis for the Flow of a Nanofluid between Rotating Parallel Plates, *Aerospace Science and Technology*, *46* (2015), Oct.-Nov., pp. 514-522
[30] Khan, U., *et al.*, Thermo-Diffusion Effects on MHD Stagnation Point Flow Towards a Stretching Sheet in a Nanofluid, *Propulsion and Power Research, 3* (2014), 3, pp. 151-158
[31] Jha, B. K., *et al.,* Natural Convection Flow of Heat Generating/Absorbing Fluid near a Vertical Plate with Ramped Temperature, *Journal of Encapsulation and Adsorption Sciences, 2* (2012), 4, pp. 61-68
[32] Makinde, O. D., Mhone, P. Y., Heat Transfer to MHD Oscillatory Flow in a Channel Filled with Porous Medium, *Romanian Journal of Physics*, *50* (2005), 9-10, pp. 931-938
[33] Said, Z., *et al.*, Mixed Convection Heat Transfer of Nanofluids in a Lid Driven Square Cavity: A Parametric Study, *International Journal of Mechanical and Materials Engineering (IJMME), 8* (2013), 1, pp. 48-57

Paper submitted: July 30, 2015
Paper revised: January 15, 2016
Paper accepted: February 26, 2016

© 2017 Society of Thermal Engineers of Serbia.
Published by the Vinča Institute of Nuclear Sciences, Belgrade, Serbia.
This is an open access article distributed under the CC BY-NC-ND 4.0 terms and conditions.